

# Protein Aggregate Identification with FMM: Rapidly Distinguish Protein from Non-Protein Particles in Biologic Formulations

## Introduction

Subvisible particles (1  $\mu\text{m}$  – 100  $\mu\text{m}$ ) are a critical quality attribute for biologics and an indicator of stability. The presence of protein aggregates can limit a product's shelf life and are a key indicator of the potential immunogenicity of a drug. The FDA suggests that, "strategies to minimize aggregate formation should be developed as early as feasible in product development."<sup>1</sup> Subvisible particles can come from several sources: (1) aggregation of the protein API, (2) degraded excipients and other particles present in the container system, or (3) manufacturing, packaging and other external contaminants<sup>2</sup>. Identifying and quantifying the inherent particle population is crucial to monitoring stability and promoting long term-efficacy.

Current subvisible analysis techniques make accurate particle identification virtually impossible. Light obscuration (LO) is a low refractive index contrast particle counting method which cannot distinguish between different particle types. Flow imaging (FI) techniques provide more information than LO, including particle images, morphological parameters and optical characteristics of particles. However, none of these features definitively identify the type of particle imaged. Flow imagers for example cannot distinguish between plastic, protein,

and degraded polysorbate which are all very similar in morphology. Technologies available for detailed chemical composition ID such as Raman microscopy/spectroscopy have been used to fill in the gaps left by particle counters; however, they are tedious, require lots of expertise and extensive signal processing, and have the throughput of a single particle per several minutes of use, making the technique useful only to expert users during failure mode analysis.

In order to fully characterize particulates and aggregates in biopharmaceutical product formulations, further information about the identity of all the particulates is crucial. Regulatory agencies expect drug manufacturers to move away from simple counting techniques and apply multiple and orthogonal methods to complement compendial methods.

In this application note we introduce Fluorescence Membrane Microscopy (FMM). FMM, exclusively available in the Aura™ system, is a high throughput, low volume, subvisible particle identification technology. FMM enables ultra-fast, 100% sampling efficiency, characterizing all particles from a single protein aggregate to tens of millions of particles in an entire multi-sample formulation, in under two hours.

## Fluorescence Membrane Microscopy

Fluorescence membrane microscopy (FMM) is a novel particle identification method that builds on Backgrounded Membrane Imaging (BMI) to identify, categorize, and further scrutinize the most common particles in an entire bioformulation sample by using established extrinsic fluorescent dye chemistries.

BMI, the backbone analysis technology used in the Aura and Horizon® instruments, images a 96-well membrane plate before and after sample filtration, and conducts novel, high optical contrast image analysis to resolve particles from 1  $\mu\text{m}$  to 5 mm in size, with a large  $>3^6$ /mL counts dynamic range. Using fluorescent dyes, biopharmaceutical particles are stained and analyzed with FMM to confirm and quantify their presence. To enable FMM, Aura uses new membrane plates specifically manufactured to support labeled fluorescent workflows.

With BMI, the software knows where every particle resides on the membrane, and most importantly all the relevant particle information from counts, sizing, morphology, and light scattering intensity is extracted from what is known as the “particle mask”. In FMM, Aura measures the fluorescence signatures only where a particle has first

been detected and measured (sized and counted) using BMI, using the fluorescence information for chemical identification only as shown in Figure 1 below. Particles that exhibit fluorescence significantly above the dark fluorescent background from the membrane plates, can then be specifically identified as protein, as is elaborated below.

## FMM Workflows

There are two main particle fluorescent staining approaches in FMM:

### 1 Solution Phase Staining: labeling the particles in solution

Most traditional fluorescence experiments are conducted in solution. However, this approach presents important drawbacks from a particle analysis standpoint: labeling the particles in solution dilutes the sample and introduces buffer and dye chemistries that may impact the sample’s chemical properties and stability. Solution staining chemistries can be very invasive, particularly if the matrix solution is nonpolar. In addition, fluorescent incubation times can be prohibitively long and limit real time use.

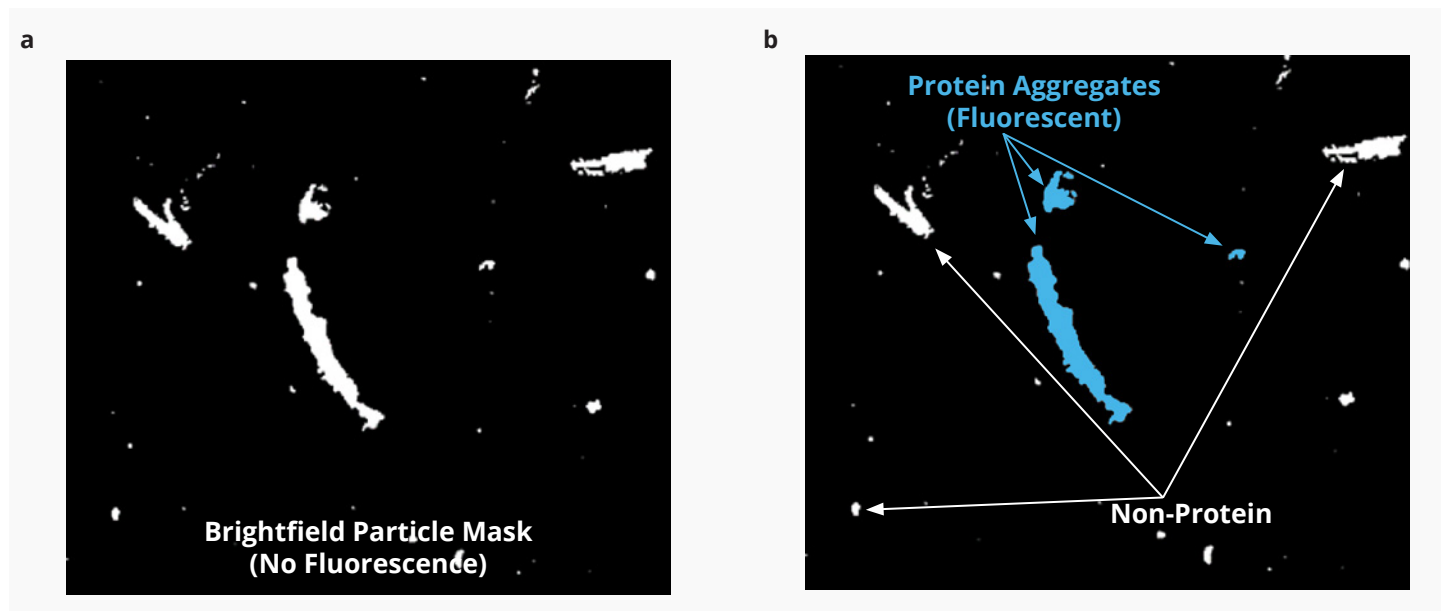


**FIGURE 1:** The Particle Mask and FMM: (a) Brightfield particle mask characterizes entire particle distribution (size and counts). Black region denotes no particles measured; white regions denotes measured particles in BMI. (b) FMM conducted after fluorescently labeling proteinaceous particles in a protein/non-protein mix.

## 2 Membrane Phase Staining: labeling the filtered particles on the membrane

Membrane Phase Staining is the fluorescent labeling of particles previously captured on the membrane surface. Applying a fluorescent label after sample filtration has many advantages. FMM can be run on particles previously measured on the membrane with BMI, which is a well-established particle measurement method that builds from USP 788 Membrane Microscopy Method 2. This allows FMM fluorescent analysis to be conducted only on “real particles” measured in brightfield, completely decoupling the impact of the fluorescent chemistry from the brightfield particle detection where the true sizing and counting of the particles is done. This allows one to conduct traditional BMI analysis, and if the user wants to ask additional questions of the particle or sample’s composition, FMM can be used. This workflow is shown in Figure 2.

Steps 1 through 3 in the workflow are the same steps as BMI where all the particle counting and sizing takes place. The fluorescent dye is then processed as shown in Step 4, after which the user reinserts the plate back into the Aura instrument for fluorescence measurement and analysis.

There are several ways in which FMM can be conducted, including hybrid methods where some of the samples can be processed using solution phase staining and others using membrane phase staining. In the case studies below, we show two different ways of conducting Membrane Phase Staining. Importantly, the user does not need to pre-specify how FMM will be conducted since the software is designed to automatically align all the fluorescent images with the corresponding brightfield images for accurate analysis.

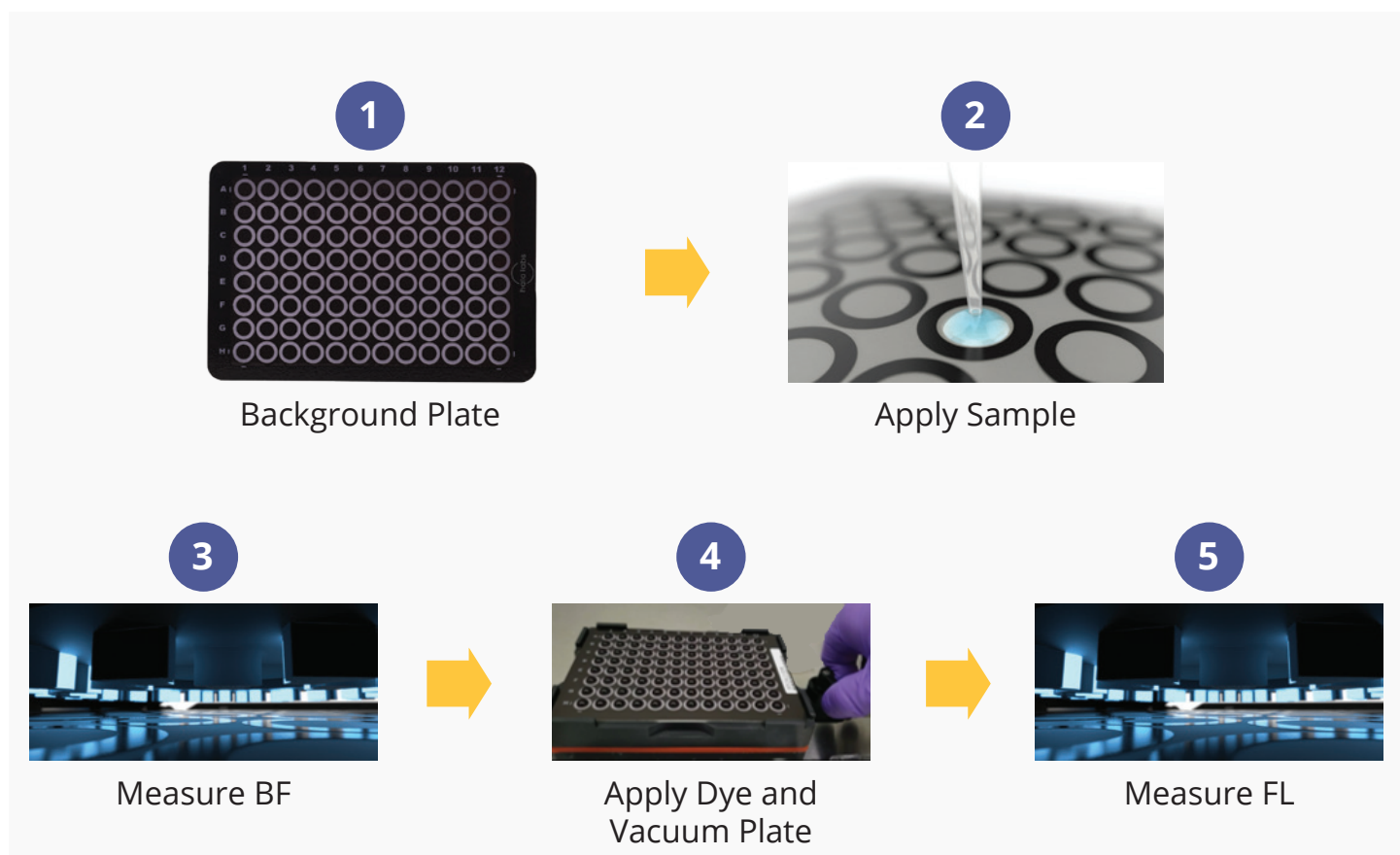


**FIGURE 2:** FMM Membrane Phase Staining Protocol. Step 1 - Brightfield background. Step 2 - Filter sample. Step 3 - Brightfield measurement. Step 4 - Apply and filter stain. Step 5 - Fluorescence measurement.

## FMM Identifies Protein Particles Labeled Using Thioflavin T

One of the most important questions in particle analysis is if a given particle or group of particles in a sample is mostly proteinaceous (the drug product) or whether the particles arise from another source. Protein vs. non-protein particle determination marks a critical junction in identifying the main underlying issues with a protein formulation and bypassing this step can result in dramatic missteps and time lost downstream.

To enable protein/non-protein determination, the first fluorescent channel in the Aura system is equipped with optics for specific protein aggregate fluorescent detection using Thioflavin T (ThT) excitation (Ex: 440/40 nm) and emission (Em: 500/40 nm) (Figure 3). Thioflavin T is a widely used, validated dye for protein aggregate fluorescent labeling and has been used in neurodegenerative disease research like Alzheimer's and Parkinson's for decades<sup>3</sup>. It specifically binds to amyloid fibrils<sup>4</sup>, misfolded Beta sheet structures that are very common amongst the highly misfolded subvisible protein aggregates. While the mechanism of how ThT binds to these fibrils is beyond the scope of this application note, as multiple mechanisms of binding have proposed<sup>5</sup>, it remains the benchmark

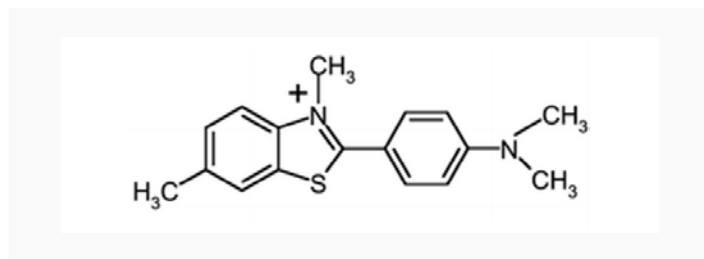


FIGURE 3: Thioflavin T Molecule.

for labeling protein aggregates. Its specificity to protein aggregates, high solubility in water, strong fluorescence, well validated body of literature and affordability make it the default protein aggregate staining dye of choice for the Aura system.

## Membrane Phase Staining Kinetics

One of the main advantages of membrane phase staining with ThT is rapid staining kinetics. Figure 4 shows membrane phase staining of hlgG aggregates that had been previously captured on a membrane. They were then labeled with 50  $\mu$ L of 5 mM ThT solution in 100% H<sub>2</sub>O, and the dye droplet was vacuumed immediately (Figure 4a) and after 3 minutes of resting on the membrane (Figure 4b).

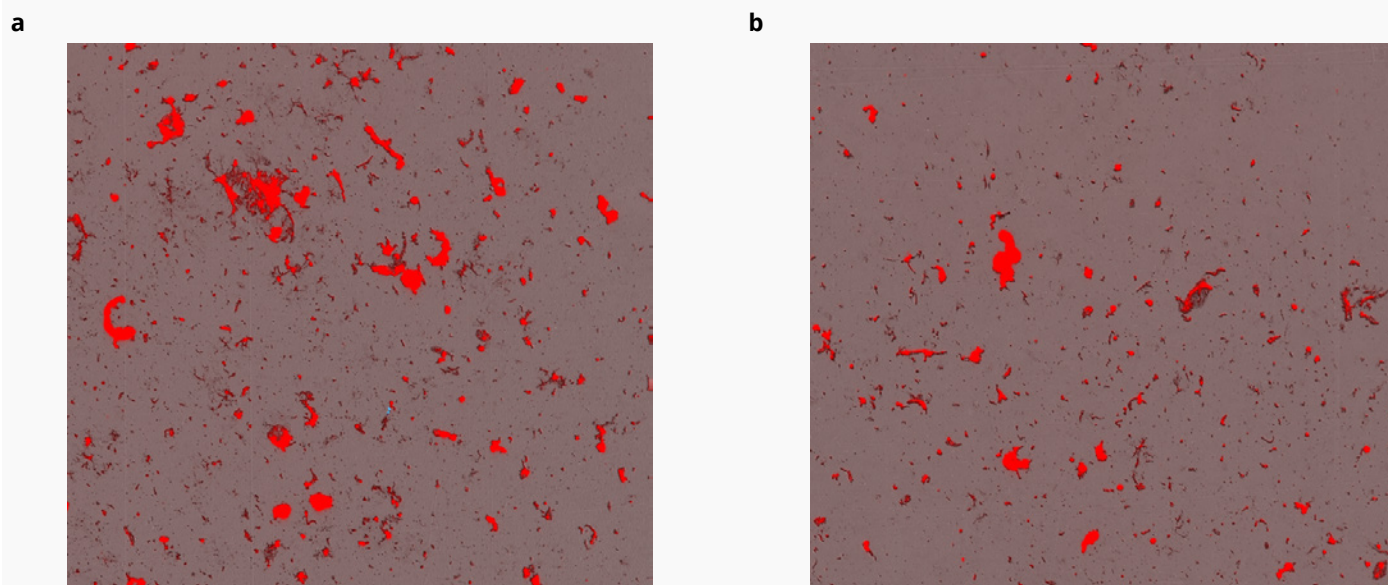


FIGURE 4: Fast staining kinetics on membrane: (a): Fluorescent hlgG aggregates (red) stained with 5 mM ThT which is immediately vacuumed, blotted and read in FMM (b) Fluorescent hlgG aggregates (red) stained with 5 mM ThT after 3 minute on-membrane incubation.

There was no measurable difference in staining efficiency between these two on-membrane incubation times. The fast staining kinetics likely results from all the particle filtrate being highly localized onto a single surface on the membrane.

## Case Study: Distinguishing the Undistinguishable to Differentiate Between hlgG Protein Aggregates and ETFE With FMM

Given the difficulty in characterizing protein aggregates, the National Institutes of Standards and Technology created a protein aggregate mimic from plastic Ethylene Tetrafluoroethylene (ETFE), Reference Material 8634, designed to mimic the morphology, particle distribution, and optical properties of common aggregated proteins. Many studies, including a detailed one by the Japanese Pharmacopeia<sup>6</sup>, have found that ETFE and protein aggregates are morphologically and optically indistinguishable using Flow Imaging (Figure 5), concluding that simple image analysis and morphology are not enough for absolute protein identity determination.

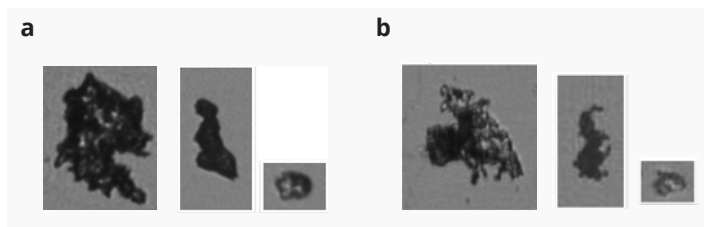


FIGURE 5: Brightfield imaging pictures of (a) protein aggregates are indistinguishable from (b) plastic ETFE particles.

### Experimental Layout

In this experiment we measure hlgG particles generated using rotational stress, ETFE particles from RM8634, and sample mixes consisting of hlgG and ETFE particles. The plate was laid out as shown in Figure 6.

### BMI Analysis of hlgG and ETFE

This experiment was conducted using the following sample and volume conditions: 24 wells containing hlgG aggregates, at 50  $\mu$ L per well, 24 wells of ETFE at 30  $\mu$ L per well, 24 wells of serially filtrated mixes of hlgG and ETFE (30  $\mu$ L of ETFE is filtered first, followed by 50  $\mu$ L of ETFE on the same wells) and 8 wells of water for injection (WFI) controls at 50  $\mu$ L each. These serial mixes enable

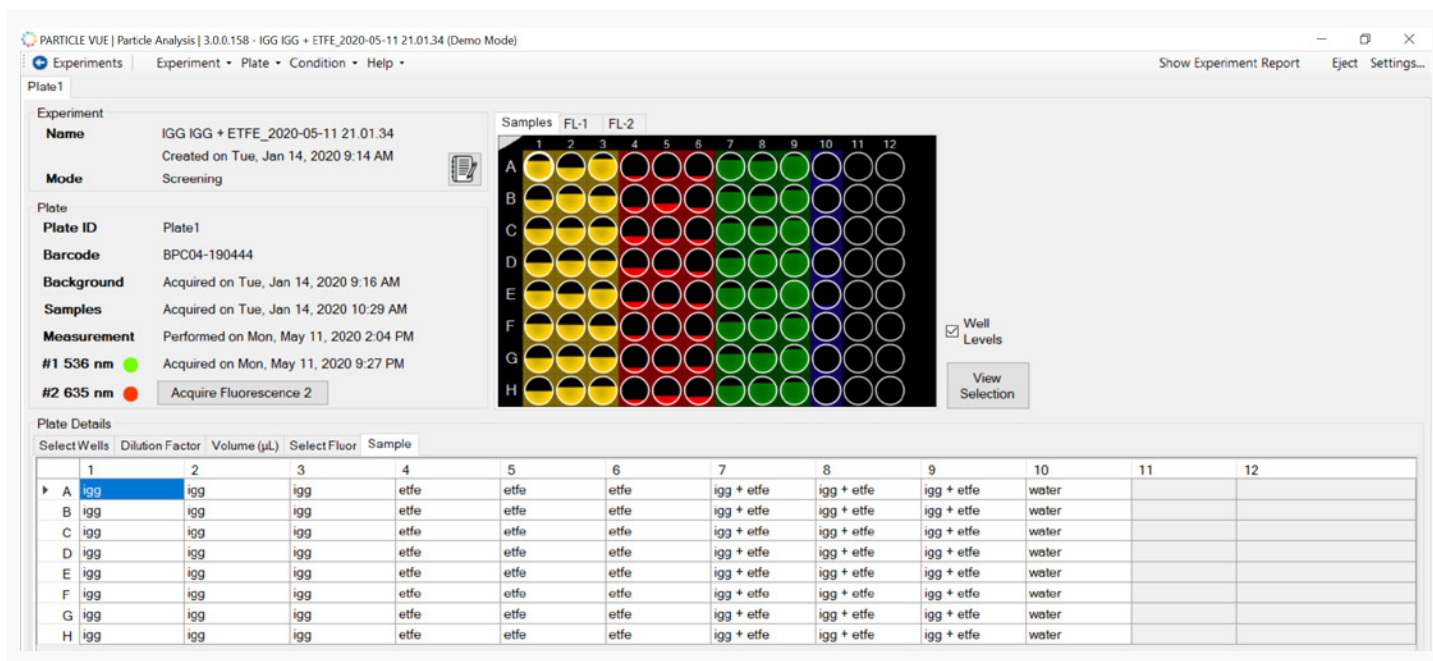


FIGURE 6: Plate layout for Protein/non-protein analysis using FMM of hlgG, ETFE, and mixed hlgG and ETFE particles.

controlled experiments as we know how much protein and non-protein particles to expect in the mixed sample, which was generated from unmixed controls with known particle counts. We can later use these count results and compare them with our FMM based protein/non-protein determination which does not use a-priori knowledge of how these particles were mixed.

As shown in Figure 7, counts/mL  $\geq 2 \mu\text{m}$  for each particle measured 49,669 for ETFE, 142,298 for hlgG and 183,997 for the serial IgG + ETFE mix respectively. With the hlgG+ ETFE particle counting standard error measuring 21,748 Counts/mL for particles  $\geq 2 \mu\text{m}$ , this experiment shows that the serial filtration mix resulted as expected: the sum of the average counts of the unmixed wells (191,967 Counts/mL  $\geq 2 \mu\text{m}$ ) is well within the error of the counts of the serially mixed wells (183,997 Counts/mL  $\geq 2 \mu\text{m}$ ).

### Fluorescent Image Analysis

We then labeled the entire plate with 5 mM ThT dissolved in WFI at 40  $\mu\text{L}$  per well. On membrane incubation

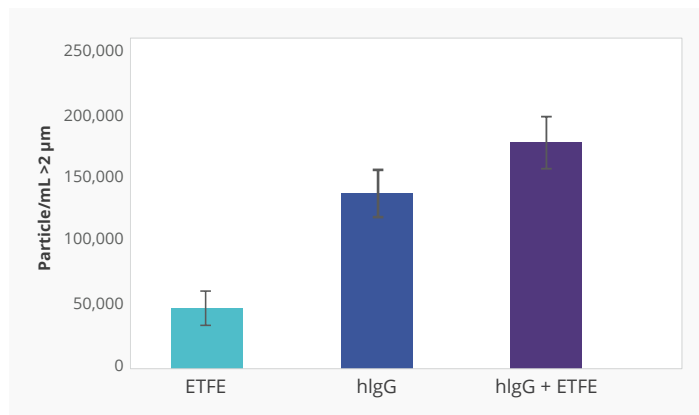


**FIGURE 7:** Particles/mL  $\geq 2 \mu\text{m}$  Counts results of ETFE, hlgG, and serial mixes of hlgG + ETFE.

was applied for 1 minute after the final ThT well was pipetted (Figure 2). After processing the dye and blotting the underside of the plate with filter paper, the plate was reinserted into the Aura instrument and the 1st Fluorescence Channel data was collected. Figure 8 visualizes wells of each of the protein (hlgG), non-protein (ETFE), and mixed components with ThT Fluorescent

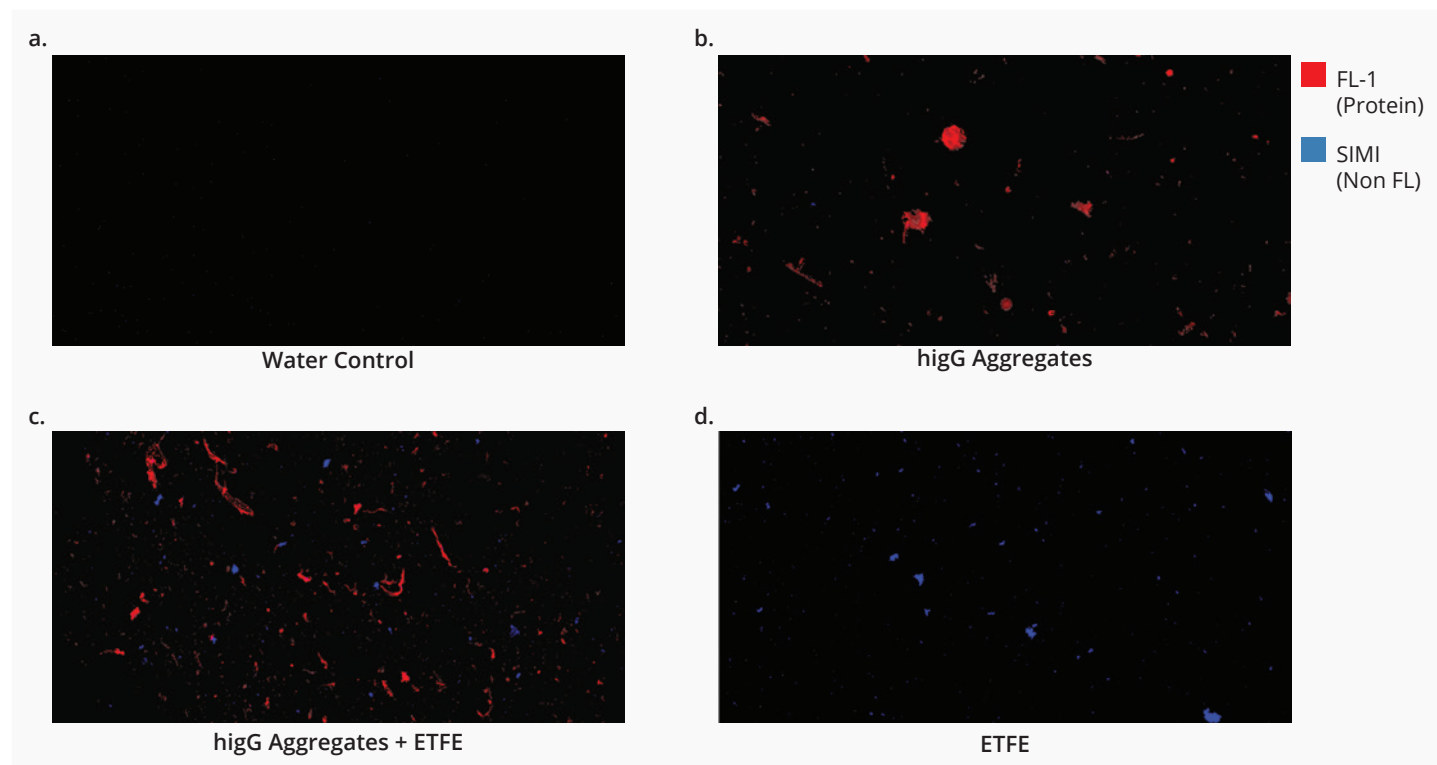


**FIGURE 8:** Alpha Blended ThT fluorescence (red) and non-fluorescent Side Illumination (blue) images of (a) WFI control (b) hlgG aggregates (c) serial mix of hlgG aggregates and ETFE and (d) ETFE particles.

excitation (Aura FL Channel 1) and non-fluorescent Side Illumination Membrane Imaging (SIMI).

As seen in Figure 8, there are no particles visible in the WFI control image (Figure 8a) in either fluorescent ThT or SIMI illumination. hIgG particles (Figure 8b) displayed both globular and fibril like morphologies from the rotational stress and exhibited very strong ThT fluorescence (red), due to the binding of ThT to the misfolded beta sheets in these protein aggregates. The hIgG particles did not scatter in SIMI (blue), indicating that these proteinaceous particles do not protrude out of the membrane plane and instead lay flat against it. ETFE particles (Figure 8d) exhibited virtually no ThT fluorescence (or intrinsic fluorescence for that matter), however scattered very strongly in SIMI (blue) indicating that these plastic particles protrude out of plane unlike the protein aggregate counterparts. Figure 8c displays an hIgG and ETFE mixed well where both the strong ThT fluorescence signature from the hIgG particles (red) and the strong SIMI scattering (blue) from the ETFE particles can be appreciated simultaneously.

## Whole well data visualization of proteinaceous and non-proteinaceous particles

Figure 9 displays particle scatter plots showing normalized average ThT Fluorescence Intensity vs. Equivalent Circular Diameter Size ( $\mu\text{m}$ ) for every particle in 3 distinct, ThT labeled wells: hIgG aggregates (a), ETFE (b) and hIgG + ETFE mixtures (d), where each dot represents a single measured particle. Figure 9a shows how labeled hIgG aggregates fluoresce in proportion to their size due to the presence of more binding sites in larger particles. Most importantly, all hIgG particles display fluorescence above the background (the 0 mark). ETFE particles in Figure 9b do not fluoresce (all dots close to the 0 FL background), indicating that ThT did not bind to ETFE. Figure 9c shows a scatter plot of a well containing a mixture of ETFE particles and hIgG aggregates. This figure shows that the mixed sample exhibit the aggregate properties of the unmixed samples – strong fluorescence from the hIgG particles, and a subpopulation that displays almost no fluorescence (ETFE).

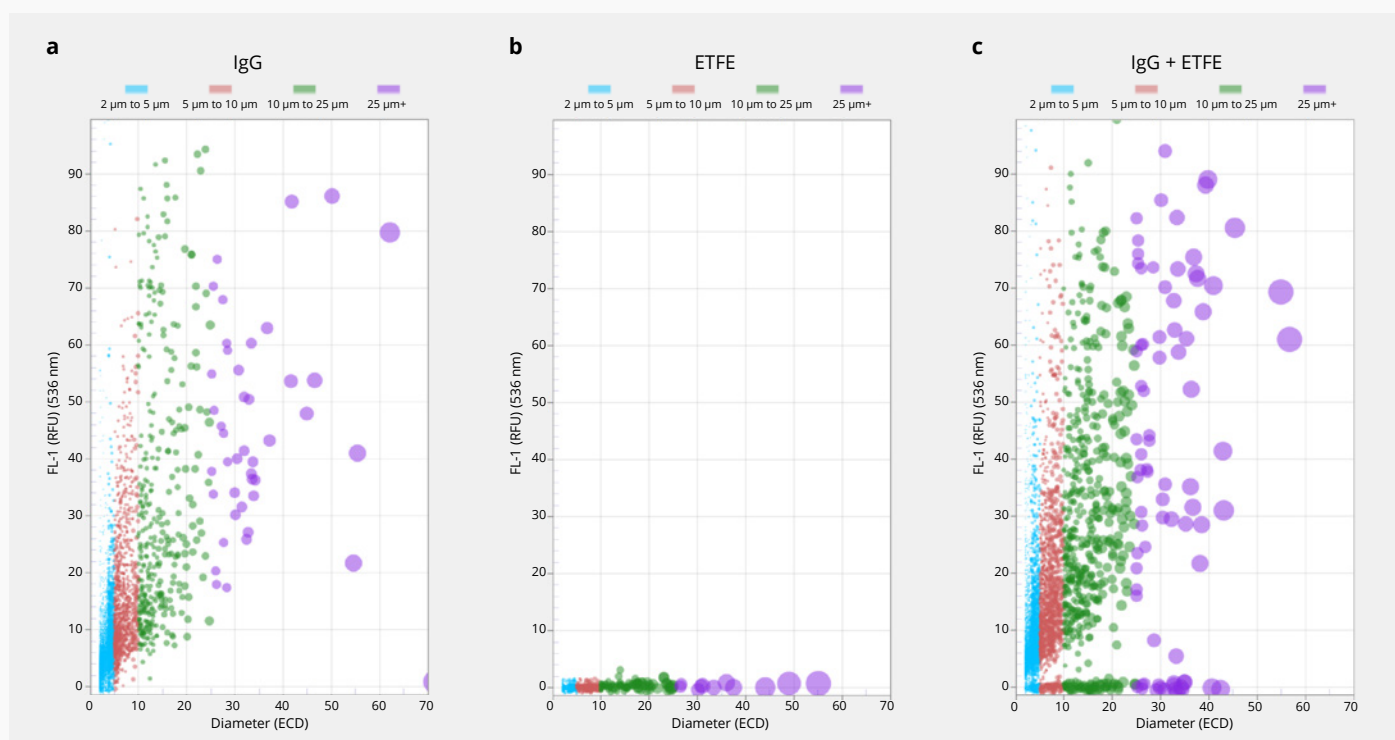


**FIGURE 9:** Normalized ThT Fluorescence vs. Equivalent Circular Diameter ( $\mu\text{m}$ ) for labeled (a) hIgG aggregates (b) ETFE and (c) hIgG + ETFE particle mixtures.

More broadly, scatter plot data visualization can be easily configured in Particle Vue software to aggregate data from select wells while plotting any particle attribute against another. Using the same selected wells from Figure 9, this 3 well data was collapsed into a single scatterplot. In Figure 10, we show Average Normalized Channel 1 Fluorescence vs. Average SIMI Intensity for every particle of these 3 wells. This figure corroborates that there are two very distinct particle populations: One that fluoresces under ThT labeling and excitation that does not protrude out of plane (no SIMI), while another population does not fluoresce after ThT labeling, but protrudes significantly out of plane, just as seen visually in Figure 8. In other words, hlgG aggregates and ETFE particles could not be any more different! Using FMM in the Aura system, we were able to distinguish them using specific fluorescence and unique geometry (SIMI), which is not possible with flow imaging.

### Analysis of mixed particles

While most of the particles in the serially mixed solution clearly showed separate subpopulations, some large particles showed intermediate SIMI and fluorescence intensities, indicating that they might have both protein and non-protein components. One such mixed particle is shown in Figure 11. Figure 11a shows the brightfield difference image for this particle, Figure 11b the SIMI intensity image, Figure 11c the fluorescent image, and Figure 11d the combined SIMI and Fluorescence alpha blended image. Out of plane features (strong SIMI) are characteristic of the left-hand side of the particle (ETFE), and ThT fluorescence on its right-hand side (hlgG aggregate portion), while the particles around it show unmixed characteristics.

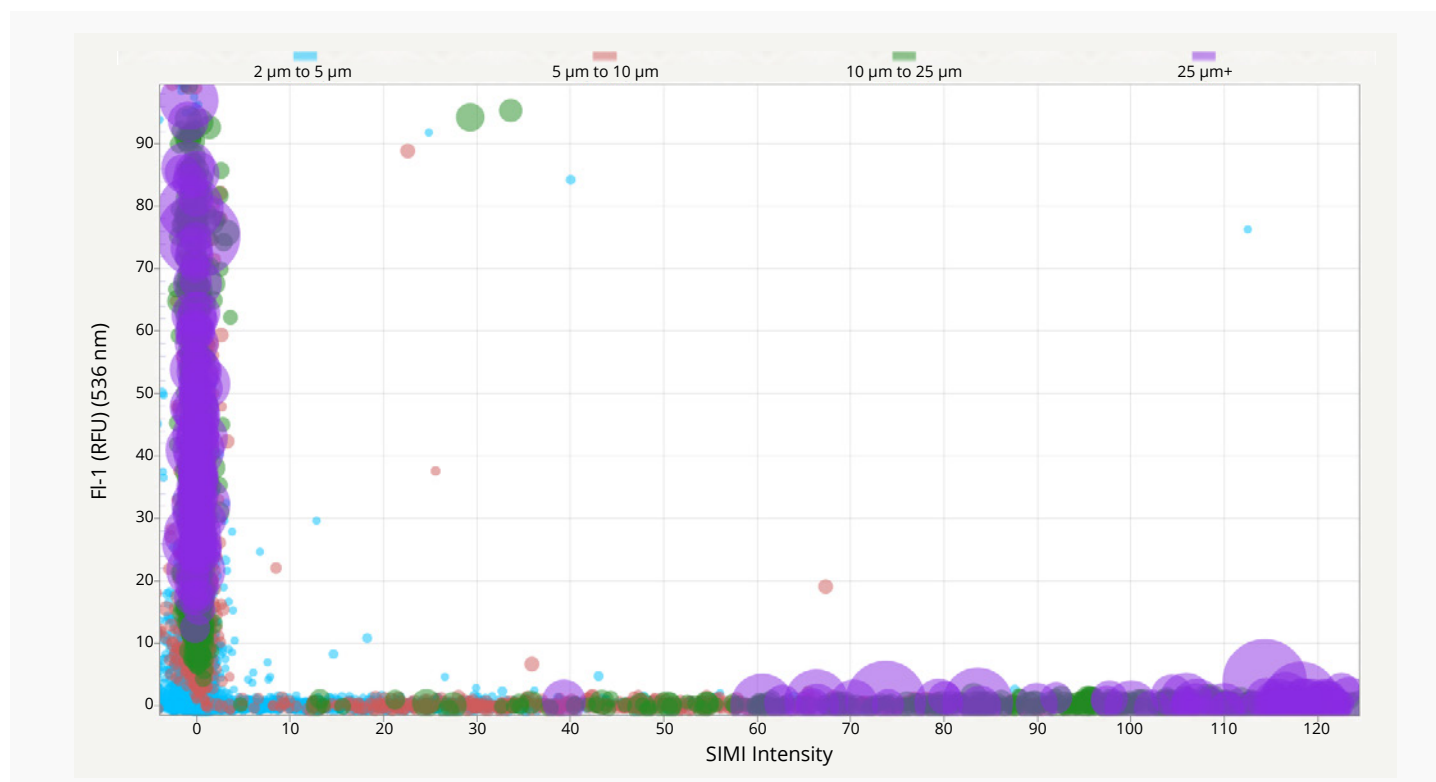
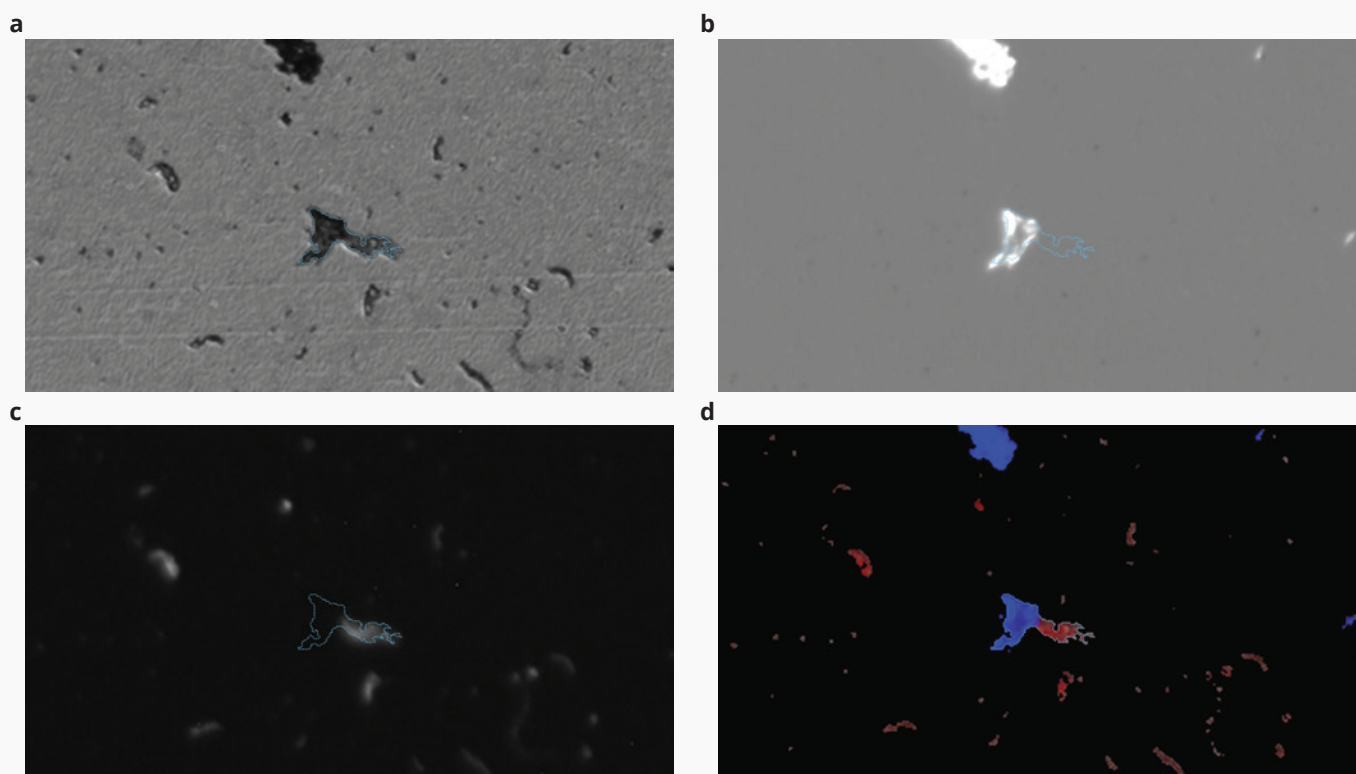


FIGURE 10: Fluorescence vs. SIMI collapsed multi-well data of hlgG aggregates and ETFE particles.



**FIGURE 11:** A mixed ETFE and hIgG particle imaged via (a) Brightfield difference (b) SIMI intensity (c) Fluorescence intensity signature and (d) Combined SIMI and Fluorescence alpha blended image.

### FMM Statistical Analysis for Protein/ Non-Protein Determination for the Entire Experiment

Particle Vue software also allows total statistical analysis for protein/non- protein determination from a single particle, to a single well to an entire experiment for high level insights. This is done using two methods: (1) Manual Threshold analysis and (2) Expression Engine based analysis. While both methods are implemented differently, they are both based on establishing a fluorescence intensity baseline (threshold) for which a particle above this baseline will be considered labeled (in the case of ThT fluorescence - a protein aggregate) or below it and therefore not labeled (not a protein aggregate).

### Manual Thresholding

Using the Manual Threshold option in the scatterplot, the data can be split into four separate quadrants. This is done by manually selecting an x-axis threshold and a y-axis threshold, both denoted with dotted lines in Figure 12. In this case, the data was split by ECD >5 μm in

the x-axis and normalized fluorescent threshold intensity of 3 – an intensity well above the background fluorescence exhibited by the membrane and the non-fluorescent ETFE particles, in the y-axis. These thresholds were then locked in the software (locking the axis for comparison as well as the thresholds), which then split the particle data into four quadrants as shown in Figure 12. For threshold data locked as shown, Quadrant 2 contains all particles above 5 μm in size that exhibit strong ThT fluorescence. Particles below the horizontal threshold exhibited almost no ThT fluorescence and are likely to not be a protein particle. With the thresholds now locked, the manual threshold cumulative table outputs the data below in Table 1.

| Sample     | Replicates | %CV<br>≥2 μm | Q1    | Q2    | Q3    | Q4    |
|------------|------------|--------------|-------|-------|-------|-------|
| ETFE       | 24         | 26.35        | 192   | 254   | 32302 | 17022 |
| IgG        | 24         | 13.28        | 78470 | 48681 | 15123 | 146   |
| IgG + ETFE | 24         | 11.82        | 89000 | 64358 | 22040 | 8921  |

**TABLE 1:** Threshold quadrants for ETFE, hIgG and mixed particles.

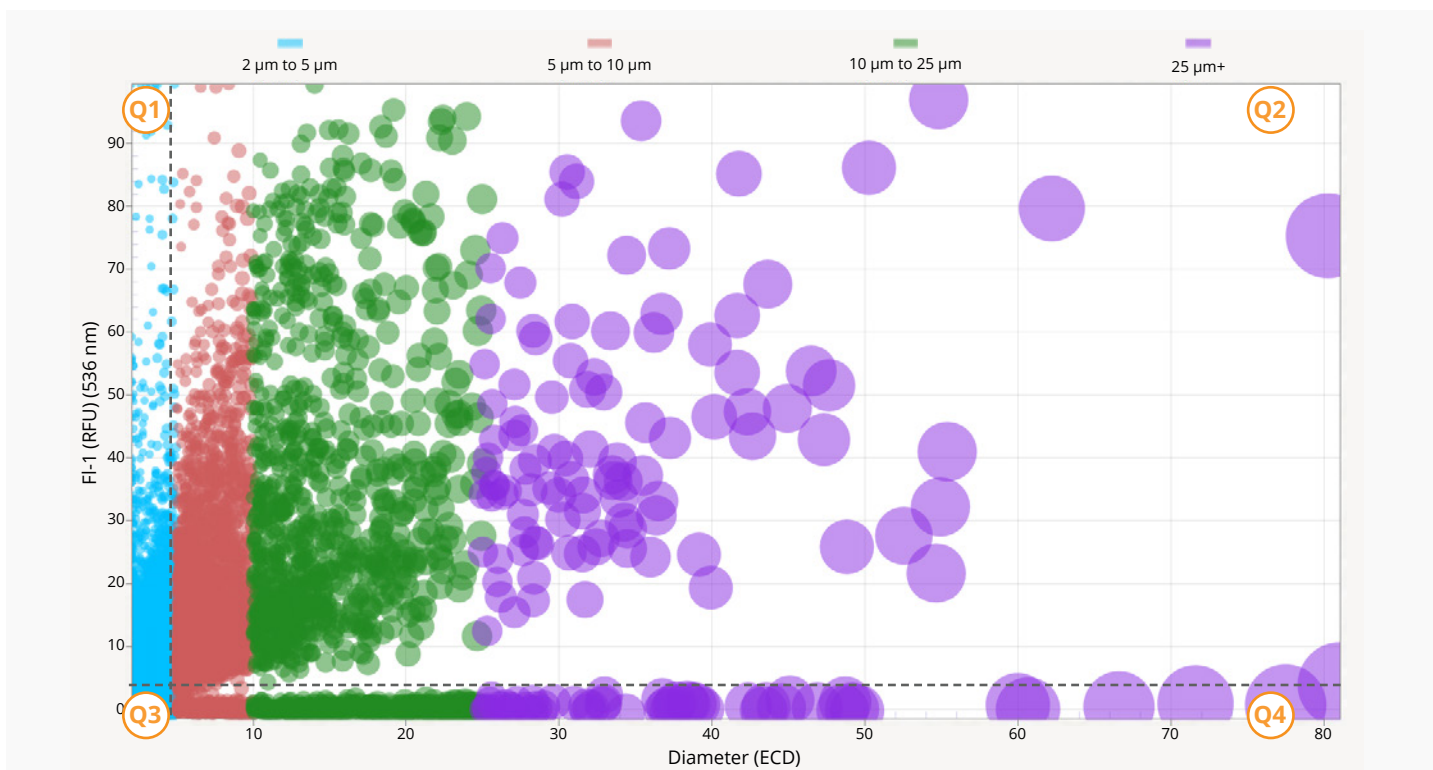


**FIGURE 12:** Manual Threshold analysis for protein/non-protein determination.

Some quick insights can be gained with the manual threshold approach: ETFE has almost no particles in Q1 and Q2, the high fluorescent quadrants, and most of its particles reside in the Q3 and Q4. For IgG aggregates, most of its particles are in the top two Quadrants where fluorescence is well above the fluorescence baseline. For a more specific and in-depth analysis, the Expression Engine is used as shown in the next section.

## Expression Engine Based FMM Analysis

One of the most powerful features of the Particle Vue software is the Expression Engine. Every particle attribute: size, morphology, SIMI and fluorescence scattering intensity, etc., is stored for every single particle in the software as shown in Figure 13. The expression engine allows one to leverage this wealth of data by querying for particles that meet desired criteria. This is done by selecting the desired particle properties from a selection table and apply Boolean logic tests to characterize the population.

For example, the expression text in Figure 13 interrogates how many particles  $\geq 2 \mu\text{m}$  in Equivalent Circular Diameter show an average fluorescent intensity in the first channel (ThT labeled fluorescence), which is 6 standard deviations above the membrane background fluorescence. If it meets the criteria, the user can be confident that the particle is proteinaceous in nature. To use the expression engine in more detail, the results from Table 2 below were obtained by creating 4 simple expressions:

- 1 Expression: Diameter >2 – Returns how many particles >2  $\mu\text{m}$  are present for every sample
- 2 Expression: FL1Intensity > FL1Background + 6\* FL1Background and Diameter >2 – Returns how many protein Particles >2  $\mu\text{m}$  are stained by ThT and are considered proteinaceous
- 3 Expression: Diameter >5 – Returns how many particles above >5  $\mu\text{m}$  are present for every sample
- 4 Expression: FL1Intensity > FL1Background + 6\* FL1Background and Diameter >5 – Returns how many protein Particles >5  $\mu\text{m}$  are stained by ThT and are considered proteinaceous

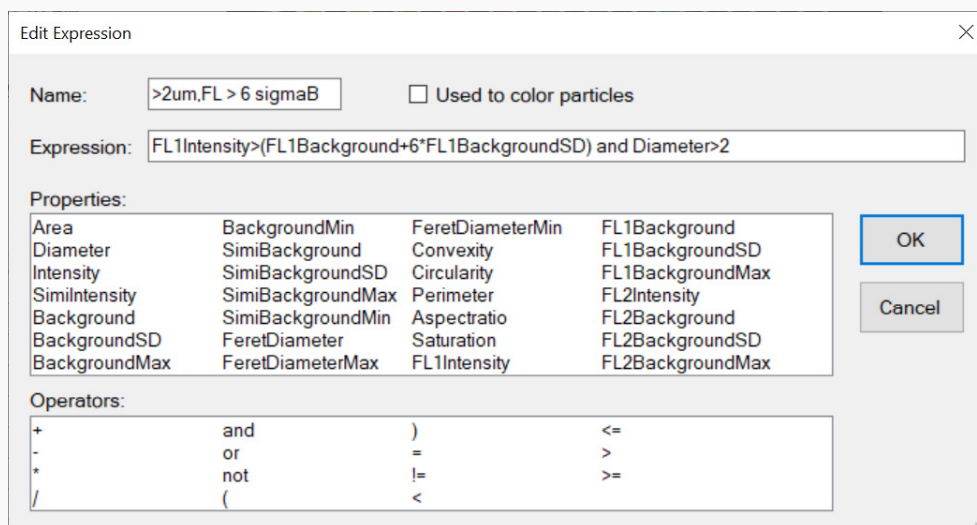


FIGURE 13: Particle Vue Expression Engine.

Table 2 summarizes the total counts for each particle type, the fluorescent counts above the background, and the percentage of the fluorescent (protein) counts of the overall population, which were directly outputted by the expression engine. ETFE particles were only mischaracterized as proteinaceous 0.9% of the time for particles  $\geq 2 \mu\text{m}$  and only 1.5% of the time for particles  $\geq 5 \mu\text{m}$ , a very low false positive rate. hIgG aggregates, on the other hand, were identified 90% of the time for  $\geq 2 \mu\text{m}$  and virtually 100% for particles  $\geq 5 \mu\text{m}$ . The presence of more binding sites (misfolded Beta sheets) in the larger aggregates likely accounts for the increased ThT fluorescence staining efficiency.

As shown in Table 2, the serial mixes of hIgG aggregates with ETFE displayed an 83.5% and 87.8% total protein component for particles for  $\geq 2 \mu\text{m}$  and  $\geq 5 \mu\text{m}$  respectively. Because this experiment was controlled, we know how much protein and non-protein particle material there was

to begin with. That means we can compare the ratio of ETFE/Mix from a particle counts standpoint and compare these results to our counts obtained via FMM analysis. In Table 3, we show that FMM did accurately predict the proteinaceous component of the mixture. The non-protein counts predicted by FMM is identical to the expected controlled counts experiment for particles above  $>2 \mu\text{m}$  and  $>5 \mu\text{m}$ .

We then subjected several non-proteins to ThT FMM. Different wells containing Palmitic Acid particles (polysorbate degradation fatty acid constituents) (Figures 14a), Corning® Cryovial Particles (Figures 14b), and Stainless-Steel Particles (Figure 14c) were all stained with 40  $\mu\text{L}$  of 5 mM ThT each and measured via the Membrane Phase Staining method shown in Figure 2. Corning cryovial delaminated particles can be easily formed by vortexing any solution in a Corning Cryovial for 1 minute, resulting in counts exceeding 30 k/mL above  $2 \mu\text{m}$ . The fluorescence

| Sample      | Replicates | ECD<br>>2 $\mu\text{m}$ (/mL) | "Protein"<br>>2 $\mu\text{m}$ (/mL) | % "Protein"<br>>2 $\mu\text{m}$ (/mL) | ECD<br>>5 $\mu\text{m}$ (/mL) | "Protein"<br>>5 $\mu\text{m}$ | % "Protein"<br>>5 $\mu\text{m}$ (/mL) |
|-------------|------------|-------------------------------|-------------------------------------|---------------------------------------|-------------------------------|-------------------------------|---------------------------------------|
| ETFE        | 24         | 49768                         | 467                                 | 0.9%                                  | 15857                         | 244                           | 1.5%                                  |
| hIgG        | 24         | 142419                        | 127865                              | 89.8%                                 | 43494                         | 43396                         | 99.8%                                 |
| hIgG + ETFE | 24         | 184318                        | 153492                              | 83.3%                                 | 66343                         | 58223                         | 87.8%                                 |

TABLE 2: Summary of particle counts, fluorescent counts and % protein obtained using the Expression Engine.

| ETFE amount in mix                      | >2 μm | >5 μm |
|---|-------|-------|
| Calculated by Counts                    | 15.5% | 14%   |
| Calculated by Fluorescence Thresholding | 15.5% | 12.2% |

**TABLE 3:** Non-protein component in mixed protein/non-protein population.

staining efficiency in ThT for particles >5 μm were below <5% for all these non-protein control particles, which can also be appreciated from the dark fluorescence images. This shows that common non-protein particles in protein formulations like plastics, polysorbates and metal have low to no cross staining with Thioflavin T, making this assay specific to protein identification.

## Conclusion

FMM using ThT allows one to conduct high throughput, low volume and specific protein/non-protein particle analysis. The power of FMM using ThT is the ability to obtain protein/non-protein ID for a whole 96-well plate assay down to a single individual particle in less than 90 minutes. ThT's high solubility and specificity to protein aggregates makes it possible to differentiate protein aggregates from particles with similar morphology and refractive index like plastics and fatty acids. Compared to spectroscopic techniques, the throughput of FMM is 1000x higher, while using best in class particle sizing and counting analysis that has its roots in the well-established membrane microscopy found in USP 788. 

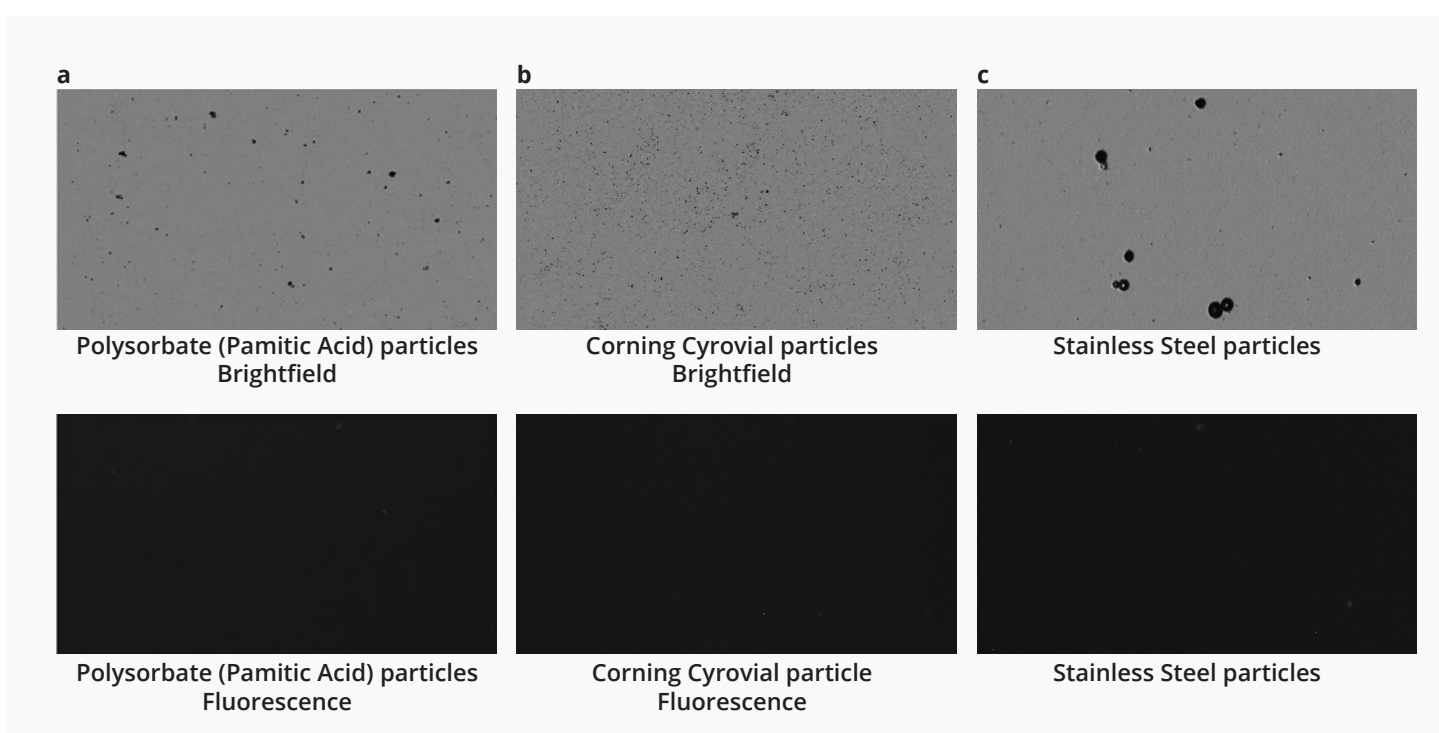


**FIGURE 14:** Negative Control: Non-proteins imaged in brightfield (BF) and 5 mM ThT stained fluorescence images (FL) modes: (a) BF difference image of palmitic acid particles (top) and FL image of palmitic acid particles (bottom). (b) BF difference image of Corning cryovial plastic delaminated particles (top) and FL image of Corning cryovial plastic delaminated particles (bottom). (c) BF difference image of 20 μm stainless steel particles (top) and FL image of 20 μm stainless steel (bottom).

## References

1. Guidance for Industry Immunogenicity Assessment for Therapeutic Protein Products. *US FDA* 2014.
2. Industry Perspective on the Medical Risk of Visible Particles in Injectable Drug Products. *Parenteral Drug Association*. 2014.
3. Naiki H, Higuchi K, Hosokawa M, and Takeda T. Fluorometric determination of amyloid fibrils in vitro using the fluorescent dye Thioflavine T. *Anal. Biochem.* 1989; 177:244–249.
4. Levine III H. Thioflavin T interaction with synthetic Alzheimers's disease  $\beta$ -amyloid peptides: Detection of amyloid aggregation in solution. *Prot. Sci.* 1993; 2:404–410.
5. Groenning M, Olsen L, van de Weert M, Flink JM, Frokjaer S, Jørgensen FS. Study of the binding of Thioflavin T to  $\beta$ -sheet-rich and non- $\beta$ -sheet-rich cavities. *J. Struct. Biol.* 2007; 158:358–369.
6. Kiyoshi M, Shibata H, Harazono A, Torisu T, Maruno T, Akimaru M, Asano Y, Hirokawa M, Ikemoto K, Itakura Y, Iwura T. Collaborative Study for Analysis of Subvisible Particles Using Flow Imaging and Light Obscuration: Experiences in Japanese Biopharmaceutical Consortium. *J. Pharm Sci.* 2019; 108(2) 832-841.

